A Molecular-Dynamics Simulation of the Complex Formation between Methyl (*R*)/(*S*)-2-Chloropropionate and Heptakis(3-*O*-acetyl-2,6-di-*O*-pentyl)-β-cyclodextrin

Jutta E. H. Köhler*[a], Manfred Hohla[a], Martina Richters[b], and Wilfried A. König[b]

Consortium für elektrochemische Industrie[a],
Zielstattstr. 20, D-81379 München, F.R.G.

Institut für Organische Chemie, Universität Hamburg[b],
Martin-Luther-King-Platz 6, D-20146 Hamburg, F.R.G.

Received June 21, 1993

Key Words: Host-guest complexes / Molecular-dynamics (MD) simulation / Enantioselective gas chromatography / Cyclodextrins

The energies of complexation of methyl (*R*)/(*S*)-2-chloropropionate [(*R*)/(*S*)-**2**] with heptakis(3-*O*-acetyl-2,6-di-*O*-pentyl)-β-cyclodextrin (**1**) and the structures of the corresponding complexes were determined by molecular-dynamcis (MD) simulations at 300 and 333 K. The geometry of the complexes, the conformations of complexed and uncomplexed **1** and (*R*)/(*S*)-**2** and the closest H–H distances between host and guest in the complexes were determined from the trajectories. The results correspond to the experimental findings from enantioselective gas chromatography.

The great progress in enantioselective gas chromatography after the introduction of modified cyclodextrins (CD) as a new type of chiral stationary phases[1] has raised many questions about the mechanism of chiral recognition and molecular interaction[2–4].

In a previous study[5] we attempted to combine information obtained from enantioselective gas chromatography, ^{1}H-NMR spectroscopy and molecular-dynamics (MD) simulations[6] to determine the structure of inclusion complexes of heptakis(3-*O*-acetyl-2,6-di-*O*-pentyl)-β-cyclodextrin (**1**) with the enantiomers of methyl 2-chloropropionate [(*R*)/(*S*)-**2**] which are resolved with a large separation factor by using **1** as a chiral stationary phase. The (*S*) enantiomer is retained on the column for a longer period. ^{1}H-NMR measurements of (*R*)/(*S*)-**2** in the presence of **1** in an unpolar solvent showed a considerable downfield shift for the resonance signals of the (*S*) enantiomer in contrast to a marginal shift of the signals of the (*R*) enantiomer. Short-time molecular-dynamics trajectories over 5 picoseconds (ps) at 300 K revealed that only the (*S*) enantiomer of **2** formed a stable complex with **1** over the whole time period when a certain initial orientation of (*S*)-**2** in **1** was chosen. In order to obtain a more detailed picture about the structural differences of the complexes of (*S*)-**2** and (*R*)-**2** with **1** we performed several trajectory simulations of the complexes and the individual components ranging up to 30 ps.

Results and Discussion

Initial Orientation of the Substrate Molecules in the Cyclodextrin Derivate

Since a detailed structure of the host-guest complexes was unknown in our previous study[5] we used two vertical orientations of (*S*)- and (*R*)-**2** in the cyclodextrin host molecule [(*S*)-UP, (*R*)-UP, (*S*)-DN, (*R*)-DN; "DN" (down) means that the methoxy group is pointing towards the narrow opening (C-6 hydroxy groups) of the cyclodextrin torus, "UP" means that the methyl group of the substrate is pointing towards the wide opening of the cyclodextrin (C-2 and C-3 hydroxy groups); see Figure 3 in ref.[5]]. These models were constructed by using the known neutron diffraction data[7] for β-cyclodextrin and by adding the side chains and the substrate as described earlier[5].

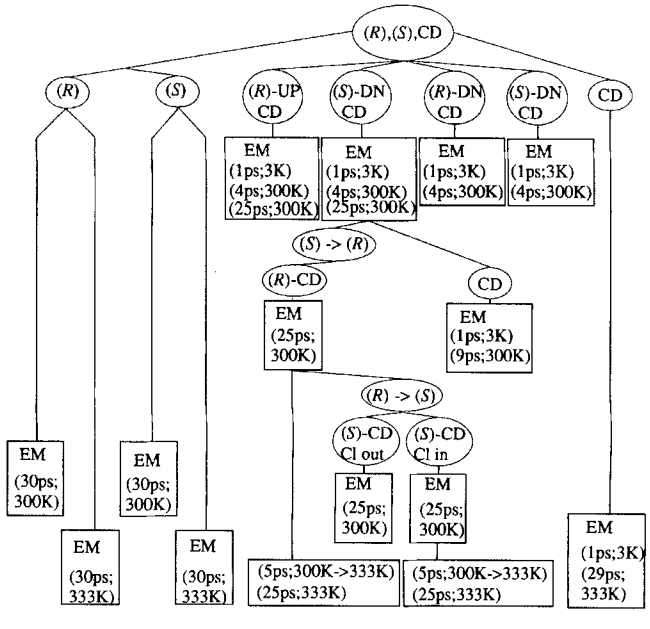

Figure 1. Scheme of the MD simulations performed (EM = energy minimization)

  0009–2940/94/0101–0119 $ 10.00+.25/0

Protocol of the Performed MD Simulations

Figure 1 illustrates the scheme of MD simulations performed.

The orientations (*R*)-DN and (*S*)-DN resulted in a fast and complete rejection of the guest molecules in less than 3 ps and were not further investigated[1]. In this study the (*R*)-UP and (*S*)-UP trajectories were elongated up to 30 ps at 300 K. While (*S*)-**2** was positioned inside of the cavity throughout the trajectory (*R*)-**2** was more loosely associated with the host molecule without leaving it completely. In this state (*S*)-**2** was exchanged for (*R*)-**2**, and the MD simulations were resumed for another 30 ps to verify the result of the first 30-ps period. Now (*R*)-**2** also preferred the interior of the cavity, and the complex displayed an even lower total energy as compared to the (*S*)-**2** complex.

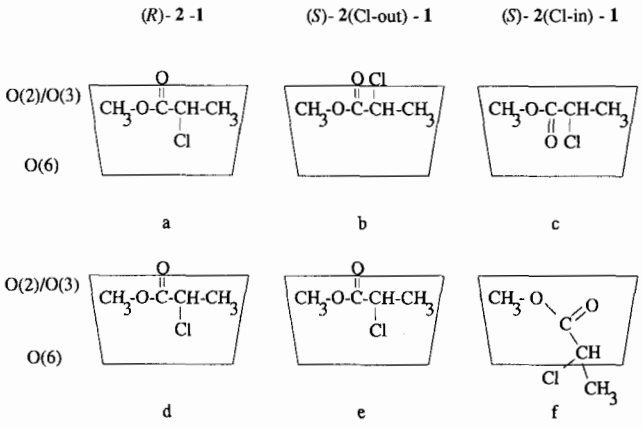

Figure 2. Scheme of the initial (a–c) and final structures (d–f) of the (*R*)-**2**–**1** complex as well as the (*S*)-**2**(Cl-in)–**1** and (*S*)-**2**(Cl-out)–**1** complexes at 300 K

Simultaneously the cyclodextrin derivative **1** [after removal of (*S*)-**2**] was submitted to another 10-ps MD simulation to obtain the energy-minimized conformation of the host molecule.

As illustrated in Figure 1, in the next step (*R*)-**2** was again replaced by (*S*)-**2**, and the MD simulation was resumed for another 30 ps with two orientations of (*S*)-**2** in the cyclodextrin cavity [(*S*)(Cl-out) and (*S*)(Cl-in) with the Cl atom of **2** pointing to the narrow C-6 opening of **1** and vice versa, see Figure 2].

Finally, the individual compounds **1**, (*S*)-**2** and (*R*)-**2** were submitted to 30-ps MD simulations at 300 K. These data were needed for the calculation of the complexation energies and for an estimation of the acurracy of the results of the MD simulations.

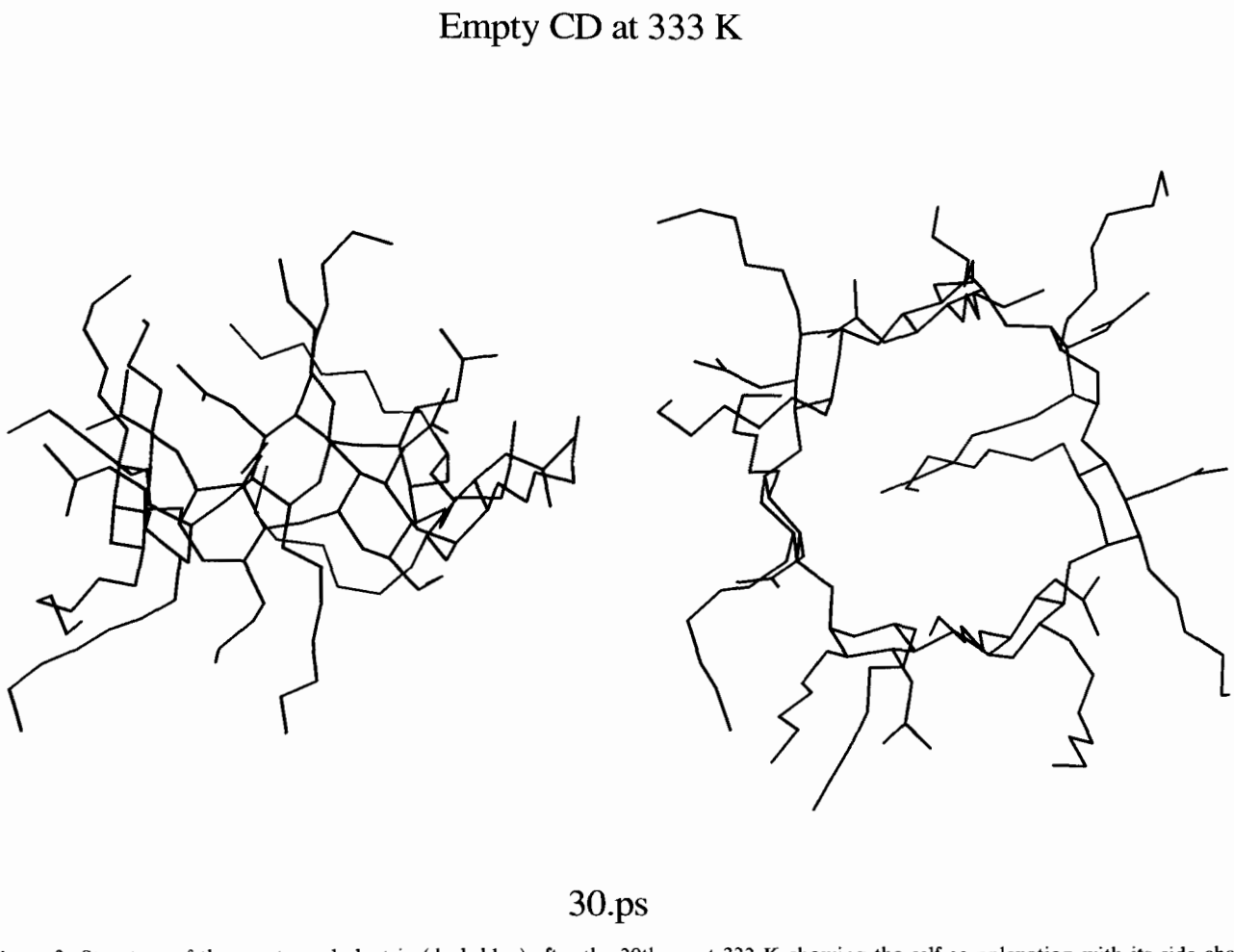

Figure 3. Structure of the empty cyclodextrin (dark blue) after the 30th ps at 333 K showing the self-complexation with its side chains (red)

To obtain an impression of the temperature dependence of the stability of the complexes the individual compounds **1**, (*S*)-**2** and (*R*)-**2** as well as the complexes were simulated at 333 K as shown in Figure 1.

Usually, a simulation period of 30 ps is not sufficient for a proper analysis of the statistical behavior of molecules. For one molecule the trajectory should be at least between 150 and 200 ps, so that the initial strain is relaxed, several movements have taken place and the equilibrium is reached. We tried to compensate for this in two ways: Firstly, analysis of our trajectories was performed in such a way that only the most reliable data could participate. Thus, we excluded the first part of the trajectories, where the molecules showed more reorientations, and averaged only the last part. Secondly, we used several starting structures and simulated them for 30 ps. The observed findings were used to select the next initial positions. This might be advantageous in cases where the general orientation of the substrate is unknown (here vertical or horizontal), since it may take some time for the complex to reorientate into correct position, or if the initial position is totally wrong, self-reorientation

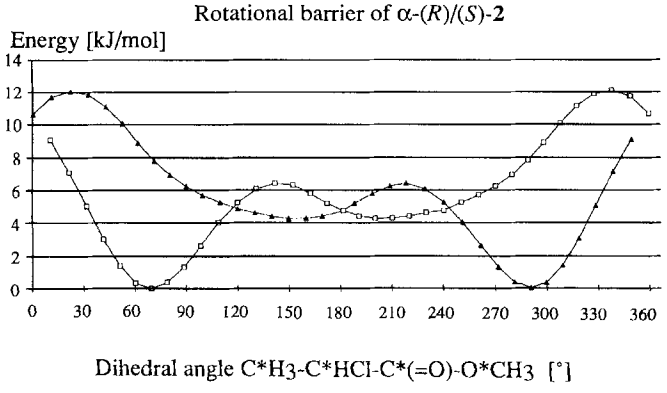

Figure 4. Rotational barrier energy curves as a function of the dihedral angle $H_3C^*–C^*HCl–C^*(=O)–O^*CH_3$ about the C-1–C-2 axis of **2** [▲ = (*R*); □ = (*S*)]

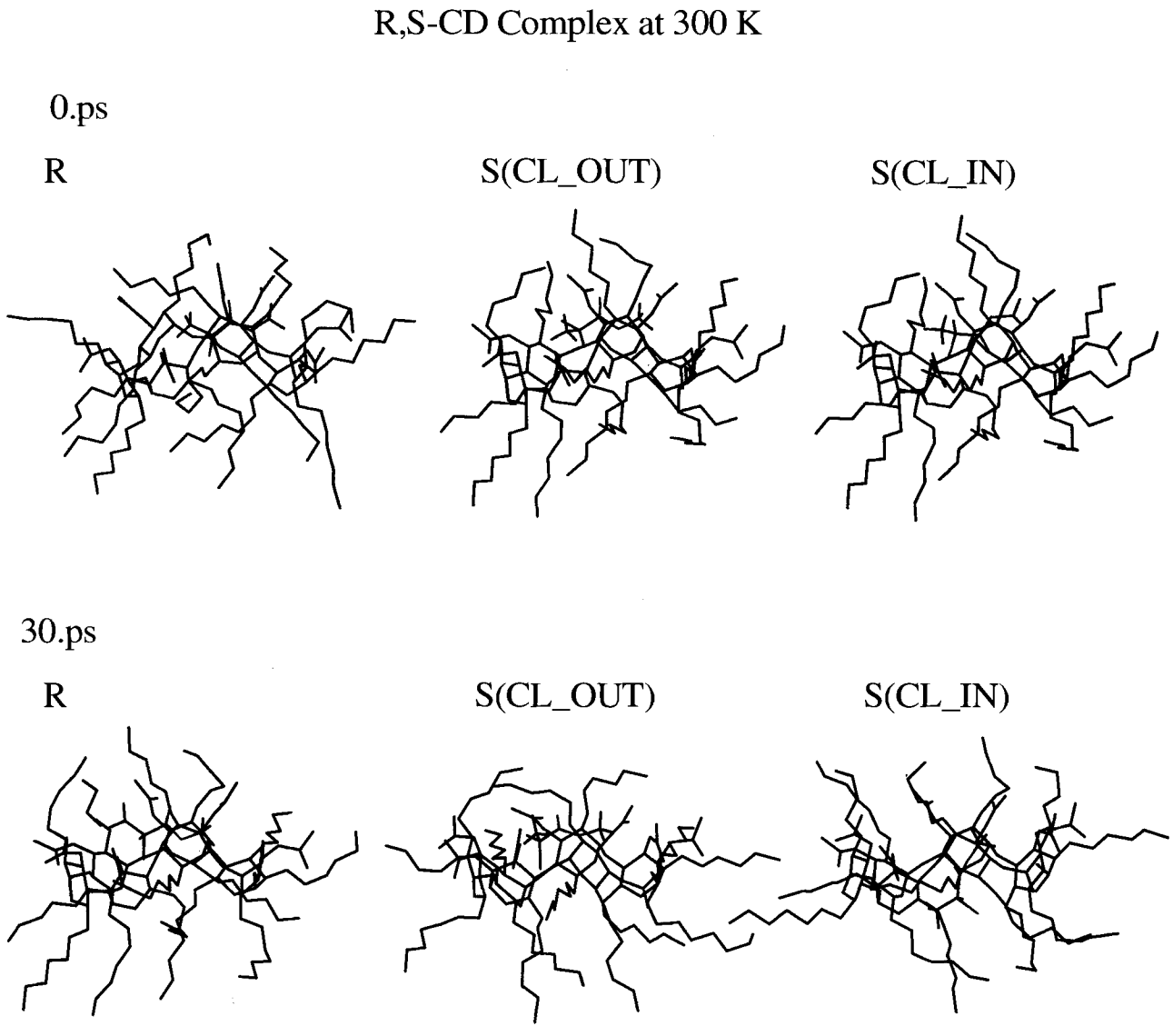

Figure 5. Initial and final structures after 30-ps MD simulation of the (*R*)-**2**–**1** complex and the (*S*)-**2**(Cl-in)–**1** and (*S*)-**2**(Cl-out)–**1** complexes at 300 K; cyclodextrin (dark blue), chloropropionate (red) with chlorine atom (green) and oxygen atoms (cyanic)

might not be possible at all (the guest molecules left the host in the first 5-ps trajectories). When starting from several initial positions, finally all trajectories should converge to the same results. In our case, we could qualitatively conclude the orientational position of **2** in **1**, since the results matched in a logical way and gave the same final results. Most probably, the numerical data might be improved when averaging would have been performed from longer trajectories. Especially in the case of the (*S*)-**2**—**1** complex at 333 K, a longer simulation time would have been advantageous, since the substrate was in an unfavorable position at the beginning and just happened to reorientate in the last part of the trajectory at about the 20th ps. Also, as known from the final results, the arbitrarily chosen initial structures for the (*S*) complexes at 300 K were less favorable than the ones chosen for the (*R*) complex.

Conformation of the Host Molecule

At 300 K approximately after the 2nd ps an acetyl substituent from the C-2/C-3 opening is approaching and intruding into the cyclodextrin cavity. This "self-inclusion" is stabilized and maintained up to the end of the trajectory. The corresponding glucose unit does not change its conformation, whereas the glucose unit adjacent to the O-4 side is deformed. The average ⟨5—10 ps⟩ potential energy between the 5th and 10th ps is 490.31 kcal/mol.

In the MD simulation at 333 K the cavity remains void up to the 7th ps. Beginning with the 8th ps one C-2 pentyl substituent is located across the C-2/C-3 opening of the cavity where it stays up to the end of the simulation. The corresponding glucose unit is deformed to a conformation between twist and boat. From the following glucose unit adjacent to C-1 a C-6 pentyl residue moves across the cavity at the narrow opening and penetrates into the cavity at the 14th ps, where it remains included up to the end of the MD simulation. The corresponding glucose unit does not change its conformation. The potential energy averages ⟨15—30 ps⟩ to a value of 516.77 kcal/mol (Figure 3).

Conformation of the Guest Molecules

Both enantiomers of **2** were submitted to 30-ps simulations at 300 K and 333 K. Although identical results would

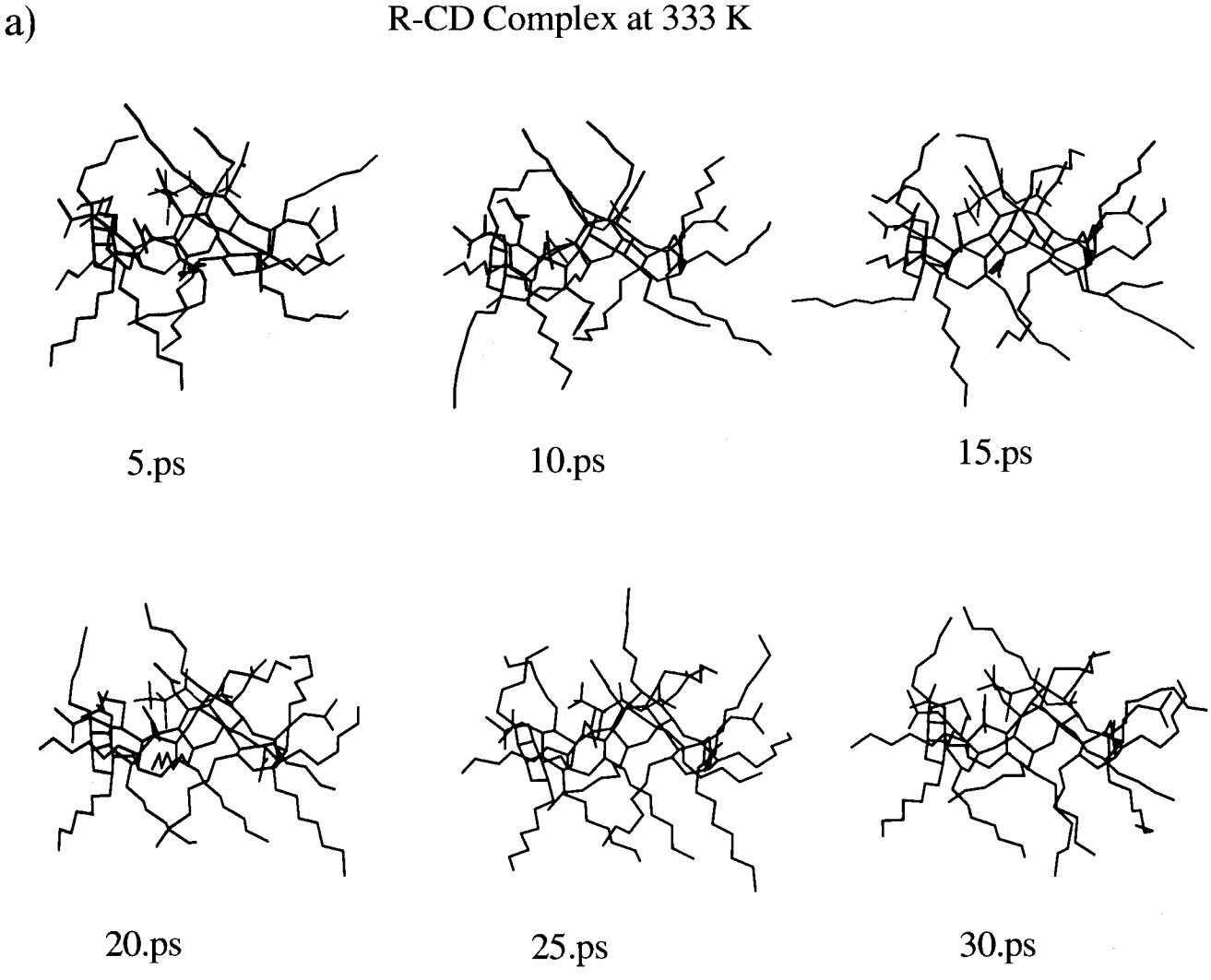

Figure 6. a) Structures of the (*R*)-**2**—**1** complexes from the MD trajectories over 30 ps at 333 K; cyclodextrin (dark blue), chloropropionate (red) with chlorine atom (green) and oxygen atoms (cyanic)

be expected for enantiomers, the MD simulations of both are considered as a test for the accuracy of the method. At slightly different average temperatures [(*R*)-**2**: 300.27 K; (*S*)-**2**: 300.43 K] the average ⟨15–30 ps⟩ potential energies were 43.35 [(*R*)-**2**] and 44.14 kcal/mol [(*S*)-**2**]. The corresponding data at 333 K were 333.54 K and 45.01 kcal/mol for (*R*)-**2** and 333.89 K and 45.06 kcal/mol for (*S*)-**2**. Typically, the deviations level off with increasing temperature.

The rotational barrier about the C-1–C-2 axis of the guest molecule **2** was calculated by using the molecular dynamics program Discover 2.6[8] as shown in Figure 4.

Orientation of the Guest Molecule in the Host Cavity

As a major result of all complex trajectories it can be concluded that the guest molecules, irrespective of the configuration, are both included in a horizontal manner in the cyclodextrin cavity. The chlorine atom is oriented towards the C-6 opening in both cases with the expected antiperiplanar arrangement of the carbonyl oxygen atom and the Cl substituent, as schematically shown in Figure 2 and in the computer graph of Figure 5.

This is proven by the result of the (*S*)-**2**(Cl-out) trajectory. After an arbitrary initial orientation of the chlorine substituent towards the C-2/C-3 opening of the cavity [(*S*)-**2**(Cl-out)] the guest molecule moves towards the C-2/C-3 rim of the cavity, reversing its position during several attempts (7th–11th ps) into a situation with the Cl substituent pointing towards the C-6 opening of the cavity (12th–17th ps). From the 18th ps the substrate slowly moves deeper into the cavity towards the C-6 opening where it remains until the 30th ps. In the case of an initial orientation of the chlorine substituent towards the C-6 opening [(*S*)-**2**(Cl-in)] no reversal of the orientation is observed.

At 300.38 K an average ⟨15–30 ps⟩ potential energy of 495.000 kcal/mol is calculated for the (*R*)-**2**–**1** complex, while for the corresponding (*S*)-**2**(Cl-out)–**1** complex at 299.95 K an average ⟨15–30 ps⟩ potential energy of 490.04 kcal/mol is obtained. The (*S*)-**2**(Cl-in)–**1** complex at 300.41 K displays an average ⟨15–30 ps⟩ potential energy of 490.85 kcal/mol.

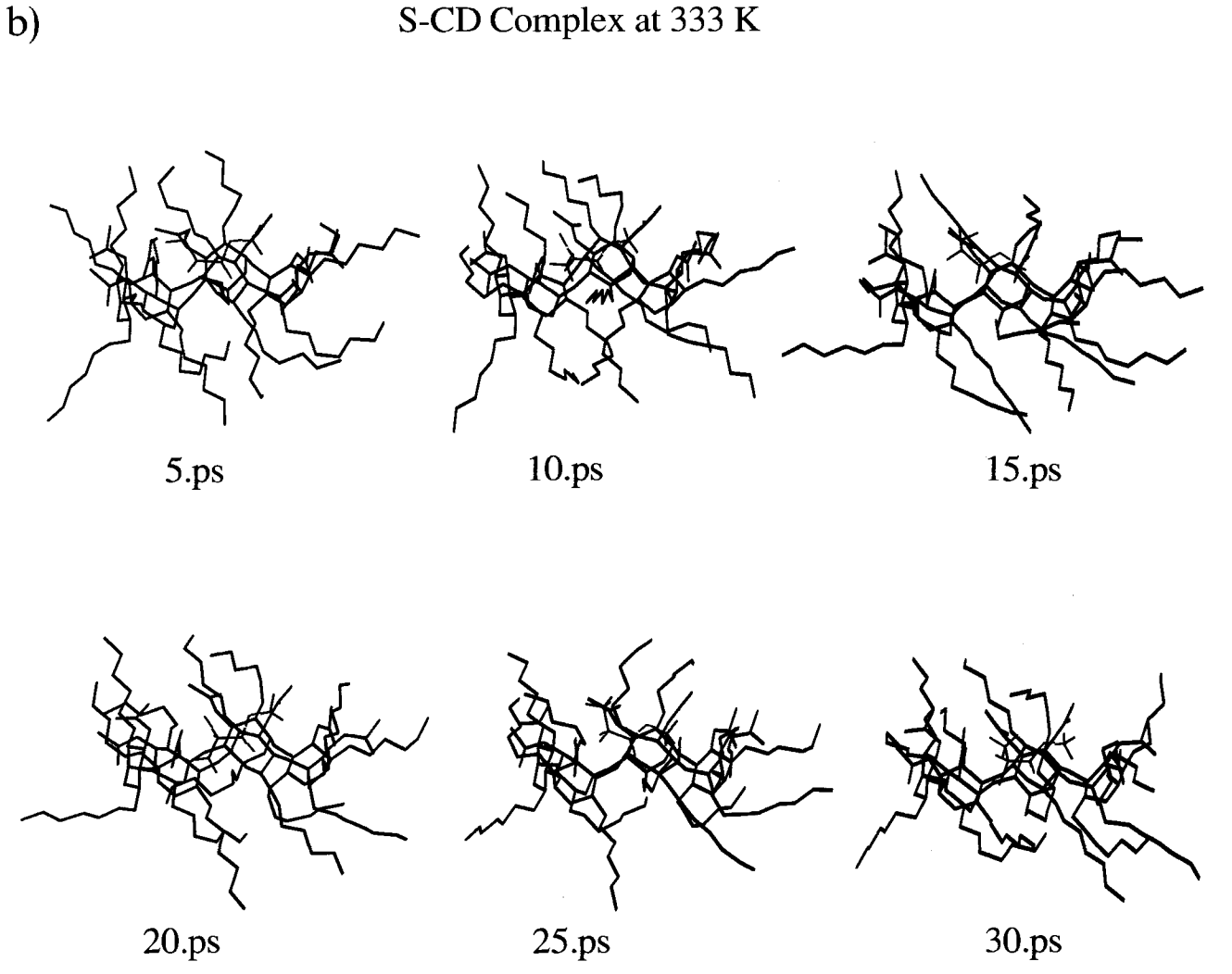

Figure 6. b) Structures of the (*S*)-**2**–**1** complexes from the MD trajectories over 30 ps at 333 K; cyclodextrin (dark blue), chloropropionate (red) with chlorine atom (green) and oxygen atoms (cyanic)

Geometry of the Host-Guest Complexes

There is no significant qualitative structural difference of the complexes at 300 K (Figure 5) as compared to the results at 333 K as shown in Figure 6.

In the host-guest complexes the cyclodextrin derivative adopts an asymmetrical shape ("induced fit"[9]). Due to the horizontal orientation of the substrate molecule with its methyl and methoxy groups forming its most distant poles, the cyclodextrin cavity displays a longer extension in just this direction, denoted as "length". The "width" corresponds to the perpendicular extension. The "length" is the average of the two averaged distances of the oxygen atoms of the glycosidic bonds of the two most remote and of the two closest glucose units in the macrocyclic system. They were determined from the trajectories of intervals between 20 and 30 ps as illustrated in Figure 7 and are given in Tables 1 and 2.

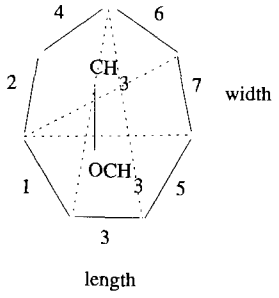

Figure 7. Measuring scheme for the determination of molecular dimensions of cyclodextrin complexes

Table 1. Averaged ⟨20–30 ps⟩ molecular dimensions [Å] of **1** and (*R*)/(*S*)-**2** and of their complexes at 300 K

Averaged distances	(*R*)-**2** - **1**	(*S*)-**2** - **1**	Empty CD Free enantiomer
CD length			
O(4,6) - O(1,3)	9.624 ± 0.354	10.573 ± 0.354	10.504 ± 0.510
O(4,6) - O(3,5)	8.647 ± 0.311	9.870 ± 0.327	10.331 ± 0.454
average length	9.136 ± 0.333	10.221 ± 0.341	10.418 ± 0.482
CD width			
O(1,2) - O(6,7)	10.534 ± 0.233	9.976 ± 0.292	9.287 ± 0.481
O(1,2) - O(5,7)	10.218 ± 0.207	9.681 ± 0.354	9.236 ± 0.454
average width	10.376 ± 0.220	9.829 ± 0.323	9.262 ± 0.468
CD total average	9.756 ± 0.277	10.025 ± 0.332	9.840 ± 0.475
Enantiomer length C(1) - C(4)	4.934 ± 0.162	4.375 ± 0.211	(*R*) 4.622 ± 0.297 (*S*) 4.608 ± 0.307

Table 2. Averaged ⟨20–30 ps⟩ molecular dimensions [Å] of **1** and (*R*)/(*S*)-**2** and of their complexes at 333 K

Averaged distances	(*R*)-**2** - **1**	(*S*)-**2**(Cl-in) - **1**	(*S*)-**2**(Cl-out) - **1**	Empty CD Free enantiomer
CD length				
O(4,6) - O(1,3)	9.755 ± 0.573	10.112 ± 0.365	9.963 ± 0.592	10.164 ± 0.927
O(4,6) - O(3,5)	8.771 ± 0.471	9.647 ± 0.319	9.186 ± 0.472	11.089 ± 0.879
average length	9.263 ± 0.522	9.880 ± 0.342	9.574 ± 0.532	10.626 ± 0.903
CD width				
O(1,2) - O(6,7)	10.642 ± 0.290	10.123 ± 0.313	10.479 ± 0.386	8.322 ± 1.150
O(1,2) - O(5,7)	10.127 ± 0.314	9.995 ± 0.242	10.003 ± 0.334	8.296 ± 0.863
average width	10.385 ± 0.302	10.059 ± 0.278	10.241 ± 0.360	8.309 ± 1.006
CD total average	9.824 ± 0.412	9.969 ± 0.310	9.908 ± 0.446	9.468 ± 0.954
Enantiomer length C(1)- C(4)	5.018 ± 0.081	4.818 ± 0.200	4.667 ± 0.229	(*R*) 4.574 ± 0.246 (*S*) 4.814 ± 0.246

The average distance of the two carbon atoms between the methyl and methoxy group of the free (*R*)-**2** is ca. 4.574 Å and it elongates to 5.018 Å in the (*R*)-**2**–**1** complex at 300 K. In the case of the (*S*) enantiomer hardly any change is seen between the free and the bound state (4.814 Å versus 4.667 and 4.818 Å, see Table 1). Uncomplexed **1** displays a higher asymmetry at 300 K as compared to the complexes.

At 333 K (Table 2) the deviation of **1** from the symmetric shape is less pronounced than at 300 K. As expected, the average distances of C-1 and the methoxy carbon atom of

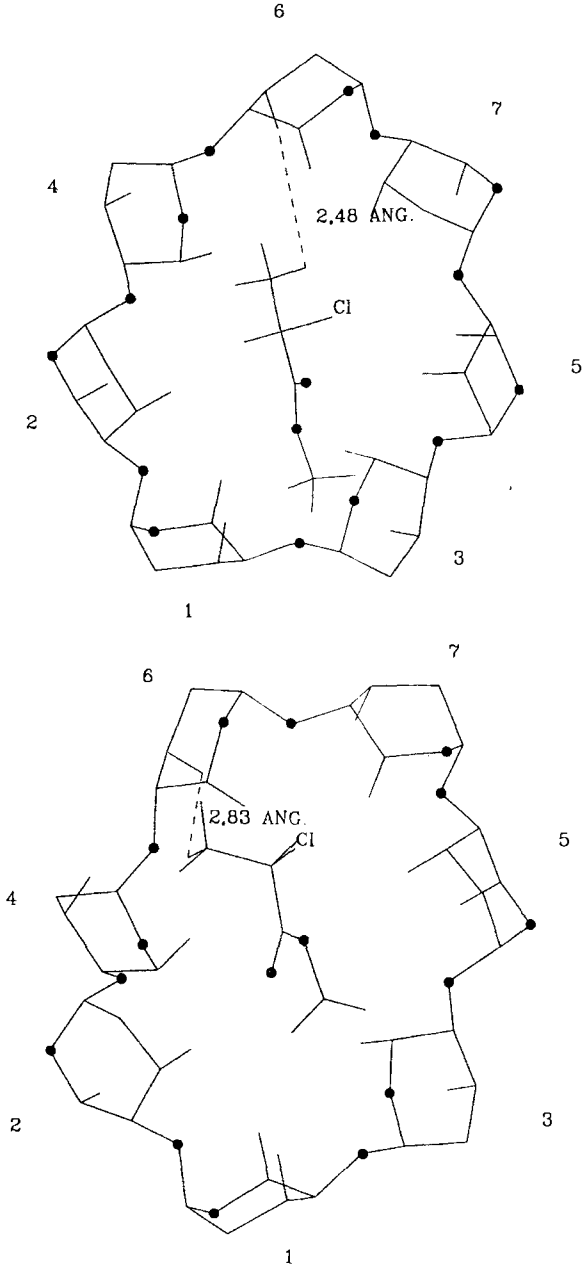

Figure 8. Short H–H distances [ANG. = Å] of (*R*)-**2**–**1** complex (top) and (*S*)-**2**–**1** complex (bottom) at 333 K (– = hydrogen atom; ● = oxygen atom)

(*R*)-**2** and (*S*)-**2** are found to be almost equal (4.622 versus 4.608 Å). In the complex, the length of the enantiomers is significantly different [4.934 Å for (*R*)-**2** and 4.375 Å for (*S*)-**2**].

Close H–H Distances between Guest and Host Molecules in the Complexes

For a comparison of the results of the NOE ^{1}H-NMR measurements of (*R*)-**2** and (*S*)-**2** in the presence of **1**[5], which indicated a close approximation of the methoxy protons and the 3-H protons of the glucose units, we have analyzed the average distances of the hydrogen atoms of the host and guest molecules in the trajectories. At 333 K there is one

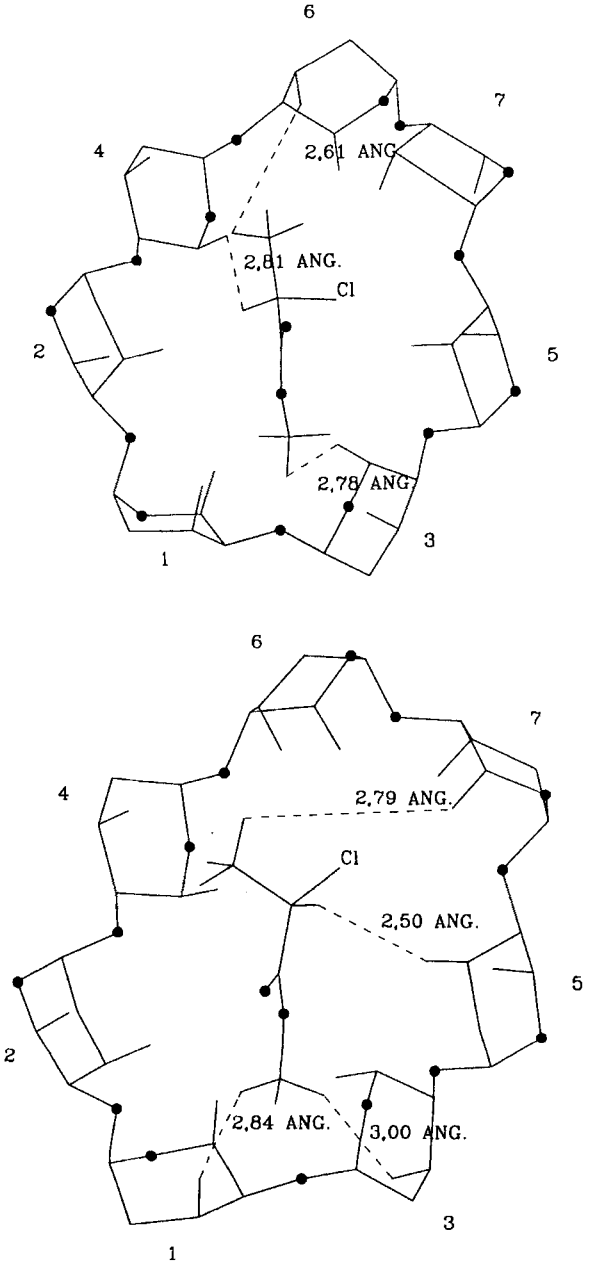

Figure 9. Short H–H distances [ANG. = Å] of (*R*)-**2**–**1** complex (top) and (*S*)-**2**–**1** complex (bottom) at 300 K (– = hydrogen atom; ● = oxygen atom)

Table 3. Averaged ⟨20–30 ps⟩ close H–H distances [Å] from the MD trajectories at 333 K

(*R*)-**2** - **1**		≤3.0	≤3.5	≤4.0	(*S*)-**2** - **1**		≤3.0	≤3.5	≤4.0
H atoms from the methoxy group of **2** and H atoms from the glucose residues of **1**									
1-H	5-H(3)	-	-	3.76	1-H	5-H(3)	-	3.49	-
1-H	3-H(3)	-	-	3.99	1-H	3-H(3)	-	3.41	-
1-H	3-H(1)	-	-	3.80	1-H	3-H(1)	-	3.17	-
2-H	5-H(3)	-	3.31	-	2-H	5-H(3)	-	-	3.54
2-H	3-H(3)	-	3.43	-	2-H	3-H(3)	-	3.21	
2-H	3-H(1)	-	-	4.00	2-H	3-H(1)	-	-	3.51
3-H	5-H(3)	-	3.04	-	3-H	5-H(3)	-	3.20	-
3-H	3-H(3)	-	3.38	-	3-H	3-H(3)	-	3.09	-
3-H	3-H(1)	-	3.28	-	3-H	3-H(1)	-	3.41	-
H atoms from the asym. center of **2** and H atoms from the glucose residues of **1**									
H	3-H(6)	-	-	3.79	H	3-H(6)	-	3.32	-
H	5-H(4)	-	3.29	-					
H	3-H(4)	-	-	3.87					
H	3-H(2)	-	-	3.54					
H atoms from the methyl group of **2** and H atoms from the glucose residues of **1**									
1-H	3-H(7)	-	-	3.84	1-H	3-H(7)	-	-	3.96
1-H	3-H(6)	2.48	-	-	1-H	3-H(6)	2.83	-	-
1-H	5-H(4)	-	-	3.92					
2-H	3-H(7)	-	3.43	-	2-H	3-H(7)	-	-	3.98
2-H	3-H(6)	-	-	3.66	2-H	3-H(6)	-	-	3.83
2-H	3-H(5)	-	3.26	-	2-H	3-H(5)	-	-	3.51
3-H	3-H(6)	-	-	3.73	3-H	3-H(6)	-	-	3.96
					3-H	3-H(5)	-	-	3.91
	average	2.48	3.30	3.81		average	2.83	3.29	3.77

Table 4. Averaged ⟨20–30 ps⟩ close H–H distances [Å] from the MD trajectories at 300 K

(*R*)-**2** - **1**		≤3.0	≤3.5	≤4.0	(*S*)-**2**(Cl-in) - **1**		≤3.0	≤3.5	≤4.0
H atoms from the methoxy group of **2** and H atoms from the glucose residues of **1**									
1-H	5-H(3)	-	3.28	-	1-H	3-H(3)	3.00	-	-
1-H	3-H(2)	-	3.26	-	1-H	3-H(1)		-	3.87
1-H	3-H(1)	-	3.42	-					
2-H	5-H(3)	-	3.50	-	2-H	3-H(3)	-	3.20	-
2-H	3-H(2)	-	-	3.83	2-H	3-H(1)	2.84	-	-
					2-H	5-H(1)	-	-	4.00
3-H	3-H(3)	-	-	3.59	3-H	3-H(3)	-	-	3.98
3-H	5-H(3)	2.78	-	-	3-H	3-H(1)	-	-	3.77
3-H	3-H(2)	-	-	3.72					
3-H	3-H(1)	-	-	3.53					
H atoms from the asym. center of **2** and H atoms from the glucose residues of **1**									
H	3-H(6)	-	-	3.97	H	5-H(7)	-	-	3.89
H	3-H(4)	-	3.45	-	H	3-H(5)	2.50	-	-
H	5-H(4)	2.81	-	-	H	5-H(5)	-	-	3.63
H	3-H(2)	-	-	3.77	H	5-H(3)	-	3.49	-
H atoms from the methyl group of **2** and H atoms from the glucose residues of **1**									
					1-H	3-H(6)	-	3.23	-
					1-H	3-H(5)	-	-	3.80
2-H	3-H(7)	-	-	3.84					
2-H	3-H(6)	2.61	-	-					
3-H	3-H(7)	-	3.26	-	3-H	5-H(7)	2.79	-	-
3-H	3-H(6)	-	-	3.80	3-H	3-H(6)	-	3.26	
3-H	3-H(5)	-	-	3.89	3-H	5-H(6)	-	-	3.60
					3-H	3-H(5)	-	-	3.71
					3-H	3-H(6)	-	3.35	-
					3-H	5-H(4)	-	3.29	-
average		2.73	3.36	3.77	average		2.78	3.30	3.81

H–H distance for both the (*R*)-**2** and the (*S*)-**2** complexes shorter than 3.0 Å between a 1-H of the guest molecule and 3-H of the host (Figure 8).

At 300 K there are four such short H–H distances in the case of the (*S*)-**2**–**1** complex, three of which between hydrogen atoms of **2** and 3-H's, and one to a 5-H of the glucose units. For the (*R*)-**2**–**1** complex only three short H–H distances were found, one to a 3-H and two to 5-H's (Figure 9).

A more complete picture of the different categories of H–H distances ($\leq$3 Å, $\leq$3.5 Å and $\leq$4 Å[10]) is given in Tables 3 and 4. These results are not in contradiction with the observed complex stabilities, although polarization effects are not accounted for in the applied force field.

Complexation Energies at 300 K and 333 K

Upon complexation of (*R*)-**2** with **1** an energy of ΔG = 38.66 kcal/mol is released, whereas in the formation of the complex with (*S*)-**2** an energy of ΔG = 44.41 kcal/mol is released. Thus, the (*S*)-**2**–**1** complex is favored by $\Delta\Delta G$ = 5.75 kcal/mol as compared with the (*R*)-**2**–**1** complex at 300 K derived from the average potential energies. At 333 K the energy difference is only $\Delta\Delta G$ = 1.12 kcal/mol [ΔG = 31.17 versus 32.29 kcal/mol for the (*R*)-**2**–**1** and (*S*)-**2**–**1** complexes, respectively]. From the gas-chromatographic separation factors of (*R*)-**2** and (*S*)-**2** (quotient of the net retention times of the enantiomers) using a 5-m capillary with **1** as a stationary phase $\Delta\Delta G$ values of 0.4 kcal/mol at 333 K and 0.65 kcal/mol at 300 K were found. Using a 20-m column, we obtained $\Delta\Delta G$ values of 0.47 kcal/mol at 333 K and 0.69 kcal/mol at 300 K. The absolute values for $\Delta\Delta G$ at a given temperature may slightly increase with increasing length of the applied column and the absolute retention times of the enantiomers. The $\Delta\Delta G$ values always increase with decreasing operation temperature of the column independent of the column length.

In conclusion, it can be stated that the trajectories over 30 ps confirm the fact that the complexation of (*S*)-**2** with the host molecule **1** is considerably stronger than the complexation of (*R*)-**2**. Moreover, a more detailed knowledge of the geometry of the complexes, the horizontal orientation of the guest molecules and the conformations of complexed and uncomplexed host and guest molecules was obtained, in agreement with experimental results.

We want to thank *A. Macri, Sr.* and *A. Macri Jr.* (München) for the documentation of the MD trajectories[11].

Experimental

All energy minimizations and MD trajectories were performed on a Microvax II computer and an Evans & Sutherlands picture system by using the Insight/Discover 2.6 programs of Biosym[8]. The CVFF force field with a harmonic potential and without cross terms and coulomb atomic charges as defined by the program were applied throughout, all 406 atoms were free to move. For the energy minimizations the steepest-descent and conjugate-gradient methods were applied. The MD simulations were carried out with the leap-frog algorithm, in vacuo, without periodic boundary conditions, with constant volume, and temperature coupling to a thermal bath (NVT ensemble). An integration step of 1 femtosecond was used. During the calculation of the trajectories every 10 femtoseconds a structure was stored for later analysis. There was practically no cut-off radius ($0.1 \cdot 10^{33}$ Å) for the non-bonded interaction.

In cases where a softer movement was required because of too much strain in the starting structures, only the temperature was reduced to 3 K for 1 picosecond, before simulating at the desired temperature of 300 or 333 K, respectively. Starting from the 30-ps structures, obtained at 300 K, we achieved a slight increase of the temperature to 333 K during 5 ps (1000 steps each at 307, at 314, at 321, and at 328 K).

From these trajectories the averaged data for the energies and temperatures were evaluated by selecting one structure per 0.02 ps (that is 50 structures per 1 ps or a total of 750 structures) within the time period from 15 to 30 ps. The averaged H–H distances from the trajectories that we compared with the NOE ^{1}H-NMR measurements were simulated with the same accuracy, they were averaged from a total of 500 structures within the time period from 20 to 30 ps. It should be mentioned here, that no NOE features (like force constants for pulling or pushing H–H distances) as provided by the Insight/Discover programs, were applied. Instead, all atoms were free to move according to the force field only[11].

[1] W. A. König, *Gas Chromatographic Enantiomer Separation with Modified Cyclodextrins*, Hüthig Buchverlag, Heidelberg, **1992**.
[2] A. Venema, H. Henderiks, R. van Geest, *J. High Resolut. Chromatogr.* **1991**, *14*, 676–680.
[3] N. Koen de Vries, B. Coussens, R. J. Meier, *J. High Resolut. Chromatogr.* **1992**, *15*, 499–504.
[4] W. Meier-Augenstein, B. V. Burger, H. S. C. Spies, W. J. G. Burger, *Z Naturforsch., B: Chem. Sci.* **1992**, *47*, 877–886.
[5] J. E. H. Köhler, M. Hohla, M. Richters, W. A. König, *Angew. Chem.* **1992**, *104*, 362–364; *Angew. Chem. Int. Ed. Engl.* **1992**, *31*, 319–320.
[6] W. F. van Gunsteren, H. J. C. Berendsen, *Angew. Chem.* **1990**, *102*, 1020–1055; *Angew. Chem. Int. Ed. Engl.* **1990**, *29*, 992–1023.
[7] C. Betzel, W. Saenger, B. E. Hingerty, G. M. Brown, *J. Am. Chem. Soc.* **1984**, *106*, 7545–7557.
[8] J. Maple, U. Dinur, A. T. Hagler, *Proc. Natl. Acad. Sci. USA*, **1988**, *85*, 5350–5354.
[9] K. Harata, K. Uekama, M. Otagiri, F. Hirayama, *Bull. Chem. Soc. Jpn.* **1982**, *55*, 3904–3910.
[10] K. Wüthrich, M. Billeter, W. Braun, *J. Mol. Biol.* **1984**, *180*, 715–740.
[11] A VHS video tape of the MD trajectories can be provided by the authors upon request.

[194/93]